



Technical Report

Shielding gas effects on flux cored arc welding of AISI 316L (N) austenitic stainless steel joints

D. Katherasan^a, P. Sathiya^{a,*}, A. Raja^b^a Department of Production Engineering, National Institute of Technology, Tiruchirappalli 620 015, Tamil Nadu, India^b Welding Research Institute, Bharath Heavy Electricals Limited, Tiruchirappalli 620 014, Tamil Nadu, India

ARTICLE INFO

Article history:

Received 9 August 2012

Accepted 6 September 2012

Available online 18 September 2012

ABSTRACT

This paper deals with the flux cored arc welding (FCAW) of AISI 316L (N) austenitic stainless steel with 1.2 mm diameter of flux cored 316LT filler wire. The welding was carried out with different shielding gas mixtures like 100% Ar, 95% Ar + 05% CO₂, 90% Ar + 10% CO₂, 80% Ar + 20% CO₂, 75% Ar + 23% CO₂ + 2% O₂ and 70% Ar + 25% CO₂ + 5% O₂ and 100% CO₂. The main aim of the work is to study the effect of various shielding gas mixtures on mechanical properties and metallurgical characters. The microstructures and ferrite content of the welds were analyzed. The mechanical characteristics such as impact test, microhardness and ductility of welds were carried out. The fracture surface impact samples were analyzed through scanning electron microscope (SEM). The fracture surface revealed a ductile rupture at room temperature and ductile rupture with a few cleavages at lower temperatures occurred. The toughness and ferrite percentages of the welds were decreased for increase of the CO₂ in shielding gas mixtures.

© 2012 Elsevier Ltd. All rights reserved.

1. Introduction

Flux cored arc welding (FCAW) has received significant attention among welders nowadays because of its advantages like easy workability and efficiency. It is suitable for mechanization and robotization and easy for applying thus providing speedy work during welding process of sheets having high thickness. It is a fusion welding process in which coalescence is produced from an arc between the work and a continuously fed filler metal electrode. The electrode core contains alloying elements that modify the molten weld metal, deoxidizers, scavenger elements that remove extra dissolved gases, stabilizers, slag forming elements and flux materials and from literatures it is evident that the use of flux wire over solid wire is more beneficial [1].

The 316L (N) austenitic stainless steel is widely used in exhaust manifolds, furnace parts, heat exchangers, jet engine parts, nuclear industry etc. The heat affected zone (HAZ) of austenitic stainless steels containing more than 0.05% C can be susceptible to a form of inter-granular corrosion called weld decay. Weld decay in austenitic stainless steels is caused by precipitation of Cr carbide at grain boundaries, which is called sensitization. Typically, the Cr carbide is Cr-enriched M₂₃C₆, in which M represents Cr and some small amount of Fe. Within the sensitization temperature range carbon atoms rapidly diffuse to grain boundaries, where they combine with Cr to form Cr carbide, so less carbon in the range of 0.03 maximum is used in 316L material [2]. Austenitic stainless

steels find applications due to excellent corrosion resistance in normal atmospheres and in a wide range of corrosive media. Type 316 steels containing 2–3% molybdenum show better general corrosion resistance as in chloride medium to pitting corrosion [3]. In 316L (N) nitrogen is added within the range of 0.06–0.08%.

The shielding gas is one of the key factors which affects the microstructure and mechanical properties of the welds. A mixture of carbon dioxide and argon is widely used as the shielding gas for FCAW process [4,6]. The percentage of carbon dioxide gas has varied from the different levels with different heat input and the effects of the welds were investigated by Yilmaz and Tümer [5]. Aloraier et al. [7] has proposed that no post weld heat treatment required for FCAW process. The welding parameters that affect weld penetration were studied by Mostafa and Khajavi [8]. Erdal Karadeniz et al. [9] studied the effect of process parameters on penetration in gas metal arc welding processes. Arivazhagan et al. [10] studied the influence of shielding gas composition on toughness of flux-cored arc weld of modified 9Cr–1Mo (P91) steel. Mohamad Ebrahimnia et al. [11] studied the effect of shielding gas composition on the mechanical weld properties of steel ST 37-2 in gas metal arc welding. In this study the influence of variation in the shielding gas composition on the weld properties of the steel ST 37-2 was investigated. Kang et al. [12] investigated the effect of alternate supply of shielding gases in austenite stainless steel GTA welding with a mixing supply of shielding gas and found that it cannot only increase the welding quality, but also reduce the energy by 20% and the emission rate of fume. To improve the efficiency of FCAW welding process the effect of carbon dioxide on the weld quality must be known. The effect of hydrogen in argon

* Corresponding author. Tel.: +91 431 2503510; fax: +91 431 2500133.

E-mail address: psathiya@nitt.edu (P. Sathiya).

Table 1
Chemical composition of base material and filler wire (weight in %).

Material	C	Cr	Ni	Mo	N	Mn	Si	P	S	Cu	Ti	Nb	Fe
AISI 316L (N)	0.024	16.89	10.07	2.16	0.0597	1.51	0.42	0.026	0.0016	0.35	0.02	0.02	Bal
316LT	0.033	18.94	11.82	2.34	–	1.18	0.62	0.022	0.008	0.10	–	–	Bal

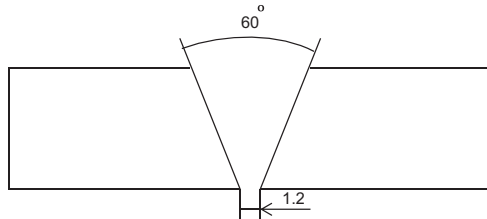


Fig. 1. Weld joint configuration.



Fig. 2. Welding setup (a – carriage, and b – gas mixer).

Table 2
Welding parameters.

Voltage	23 V
Welding current	210–220 V
Welding speed	5.5 mm/s
Wire feed rate	9.5 m/min
Transfer mode	Spray transfer mode

stainless steel was studied [14]. Some works have studied the influence of shielding gas composition on the apparent weld shape [15], on the surface tension of droplet that is travelling between electrode tip and weld pool [16], and on the mode of the droplet transfer and the amount of resulting fume [17]. It was found that small amount of oxygen added to the argon, improves the apparent shape and the droplet transfer mode [18]. However the investigation on the effects of mixtures of Ar, O₂ and CO₂ on the weld characteristics of 316L (N) is very limited. The aim of the present work is to study the effect of various mixtures of Ar, O₂ and CO₂ on microstructure, microhardness, ferrite percentage and ductility of flux cored arc welded 316L (N) austenitic stainless steel specimen. In this study welds are made on the 316L (N) material by varying the shielding gas mixture percentages namely 100% Ar, 95% Ar + 05% CO₂, 90% Ar + 10% CO₂, 80% Ar + 20% CO₂, 75% Ar + 23% CO₂ + 2% O₂ and 70% Ar + 25% CO₂ + 5% O₂ and 100% CO₂ and their mechanical and metallurgical characteristics are studied.

shielding gas was investigated for tungsten inert gas welding of 316L austenitic stainless steel [13]. The effect of shielding gas composition on weld metal nitrogen retention in 316LN austenitic

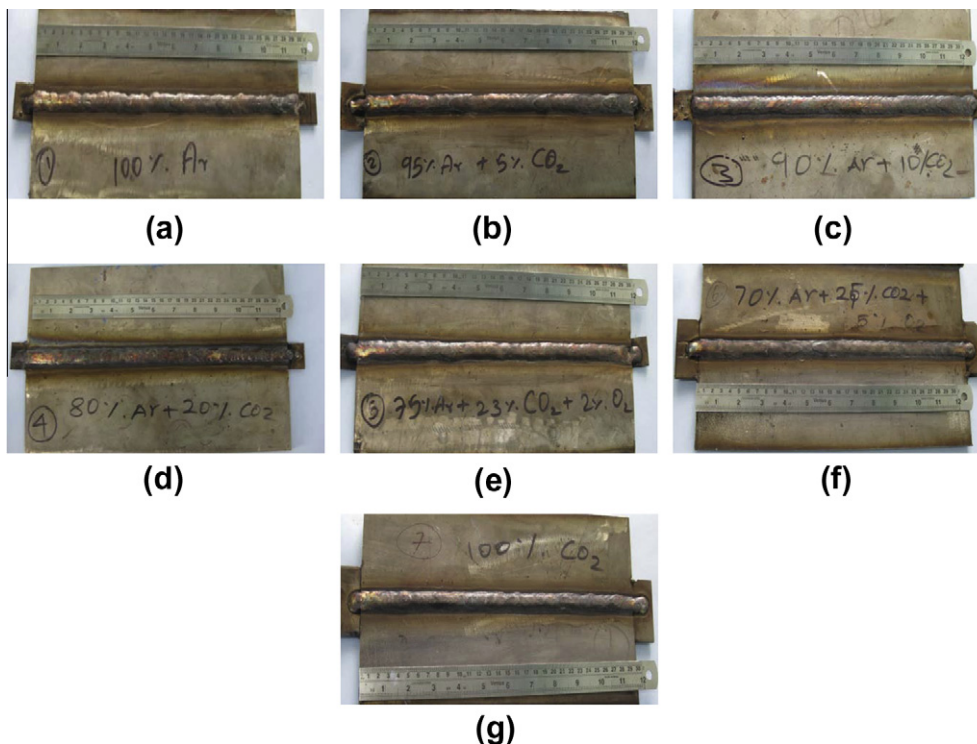


Fig. 3. (a–g) Photographs of welded specimens with different shielding gasses (a – 100% Ar, b – 95% Ar + 05% CO₂, c – 90% Ar + 10% CO₂, d – 80% Ar + 20% CO₂, e – 75% Ar + 23% CO₂ + 2% O₂, f – 70% Ar + 25% CO₂ + 5% O₂ and g – 100% CO₂).

Table 3
Oxygen potential (O_p) values for shielding gas mixtures.

Shielding gas mixtures	100% Ar	95% Ar + 05% CO ₂	90% Ar + 10% CO ₂	80% Ar + 20% CO ₂	75% Ar + 23% CO ₂ + 2% O ₂	70% Ar + 25% CO ₂ + 5% O ₂	100% CO ₂
Oxygen potential (O_p)	0	3.5	7	14	18.1	22.5	70

Table 4
Measured ferrite percentages of welds.

Shielding gas	Ferrite percentage						Average
100% Ar	9.82	9.95	9.73	9.81	9.86	9.83	9.83
95% Ar + 05% CO ₂	9.15	9.27	9.42	9.38	9.22	9.29	9.29
90% Ar + 10% CO ₂	8.52	8.76	8.91	8.66	8.59	8.69	8.69
80% Ar + 20% CO ₂	8.24	8.38	8.57	8.42	8.48	8.42	8.42
75% Ar + 23% CO ₂ + 2% O ₂	8.43	8.51	8.65	8.46	8.57	8.52	8.52
70% Ar + 25% CO ₂ + 5% O ₂	8.55	8.57	8.68	8.61	8.67	8.62	8.62
100% CO ₂	7.63	7.96	8.11	7.84	7.72	7.85	7.85

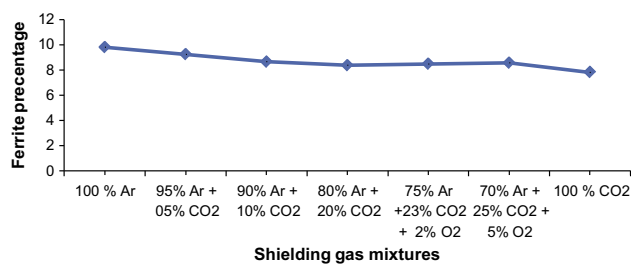


Fig. 4a. Ferrite percentages of welds.

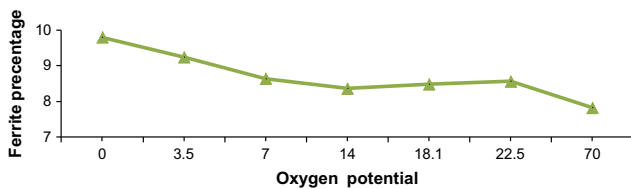


Fig. 4b. Ferrite percentages of welds as a function of oxygen potential.

2. Experimental procedure

AISI 316L (N) austenitic stainless steels were used as base material for this study. AWS 5.22 E316LT1-1/4 flux cored wire with diameter of 1.2 mm is used as filler material. The chemical composition of the base metal and filler wire is given in Table 1.

The base material is cut into the required size of $400 \times 105 \times 8 \text{ mm}^3$. V shaped groove was used and two passes of FCAW were performed using copper substrate as well. The plates were joined firstly in the root pass and then second cover pass

Table 5
Chemical composition of welds.

Shielding gas	Cr	Si	Mo	Nb	Ti	Ni	Mn	Cu	N	C	Cr-eq	Ni-eq
100% Ar	18.92	0.615	2.335	0.020	0.0200	09.58	1.49	0.29	0.048	0.024	23.697	12.332
95% Ar + 05% CO ₂	18.68	0.593	2.276	0.019	0.019	10.22	1.38	0.27	0.045	0.025	23.322	12.866
90% Ar + 10% CO ₂	18.66	0.587	2.172	0.018	0.017	10.25	1.31	0.25	0.046	0.026	23.131	12.912
80% Ar + 20% CO ₂	18.06	0.579	2.081	0.017	0.016	11.02	1.29	0.24	0.047	0.027	22.376	13.122
75% Ar + 23% CO ₂ + 2% O ₂	18.31	0.581	2.127	0.017	0.016	11.22	1.23	0.25	0.042	0.026	22.699	13.241
70% Ar + 25% CO ₂ + 5% O ₂	18.18	0.583	2.159	0.018	0.017	11.06	1.27	0.26	0.041	0.025	22.623	13.297
100% CO ₂	16.41	0.566	2.014	0.016	0.015	11.81	1.19	0.28	0.042	0.029	20.5975	13.312
Base material [316L (N)]											21.001	13.203
Filler wire [316LT]											23.695	13.431

respectively. A schematic weld joint configuration is shown in Fig. 1. Butt joint configuration was used. The welding was performed with ESAB-ARISTO machine with a power rating of 450 W and the carriage is FRONIUS-FCU-4-RC were used. The welding setup and gas mixer unit of WITT-GASTECHNIK is shown in Fig. 2a and b. The CO₂ and Ar percentages vary from 0% to 100% and O₂ vary from 0% to 40%. For all set of welding, the gas flow rate is kept as constant (20 lpm).

Prior to welding, the plates are cleaned with stainless steel brush and swabbed by acetone for cleanness. Based on the preliminary welding trials the process parameters were chosen and they are presented in Table 2. The inter-pass temperature was kept below 150 °C with the help of thermo chalk due to thermal conductivity of austenitic stainless steel. The photographs of the different shielded welds are shown in Fig. 3a–g.

The test specimens were obtained from the weld plate. The specimens were mounted later flattened and then polished using SiC abrasive paper with grit ranges from 180 to 1200. Then the samples were then lightly polished using 3 μm diamond paste. Samples were then washed, cleaned by acetone and then dried, followed by electrolytic etching in 10% oxalic acid at 9v for 30 s [19] and ASTM: E3-11. Chemical composition of the weld metal is found from spectra chemical analysis. Ferrite percentages were measured using ferrite scope and also the percentage of ferrite is calculated using Cr_{eq} and Ni_{eq} . The specimens for Charpy test were taken as perpendicular to weld direction according to the ASTM: E23 standards. The impact tests were conducted at room temperature, –100 °C and –196 °C. Micro hardness measurements were taken at parent metal, HAZ and weld zone with a load of 1kgf for 20 s during measurements. The face bend testing of the material was conducted according to ASTM: E190-92 standards to know the development of the cracks and fissures which will help to know the ductile nature of the weld material. Finally microstructural examinations were carried out at various cross sections of the weld using optical microscope.

3. Results and discussion

3.1. Oxygen potential

In general, the oxygen potential (O_p) means the oxidizing effect of the shielding gas and/or the significance of oxygen on the weld metal. Oxygen and CO₂ are oxidizing gases. They are very active at high temperature and therefore their direct chemical effect on the

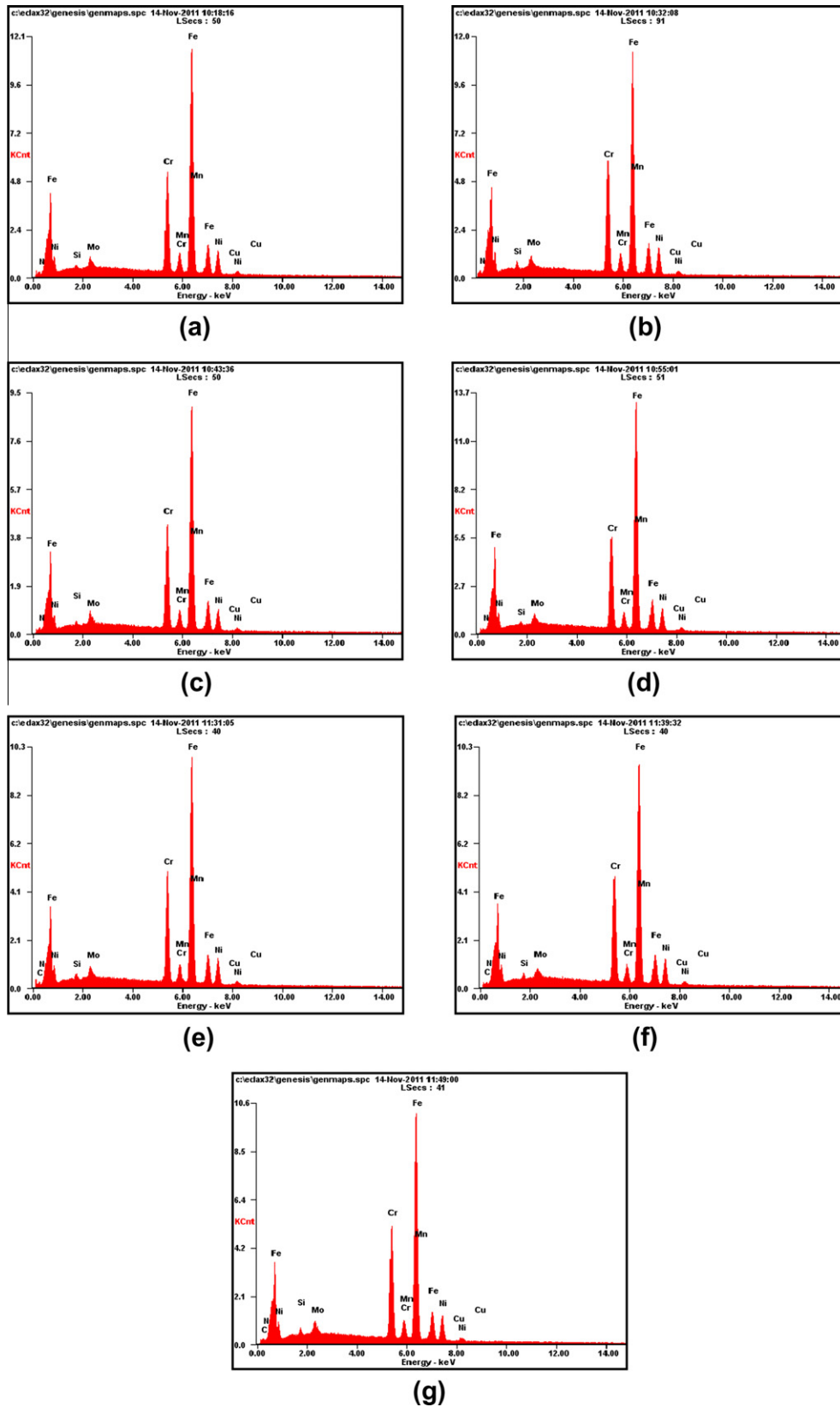


Fig. 5. (a–g) EDAX spectra of welds (a – 100% Ar, b – 95% Ar + 05% CO₂, c – 90% Ar + 10% CO₂, d – 80% Ar + 20% CO₂, e – 75% Ar + 23% CO₂ + 2% O₂, f – 70% Ar + 25% CO₂ + 5% O₂ and g – 100% CO₂).

Table 6
Predicted and measured ferrite percentages of welds.

Shielding gas	Predicted ferrite percentage	Measured ferrite percentage	% of error
100% Ar	10.4	9.83	5.48
95% Ar + 05% CO ₂	9.7	9.29	4.23
90% Ar + 10% CO ₂	9.2	8.69	5.54
80% Ar + 20% CO ₂	8.9	8.42	5.39
75% Ar + 23% CO ₂ + 2% O ₂	8.7	8.52	2.07
70% Ar + 25% CO ₂ + 5% O ₂	8.8	8.62	2.05
100% CO ₂	8.2	7.85	4.27

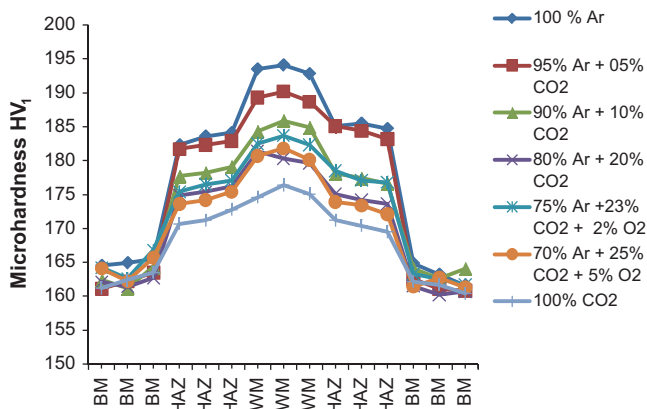


Fig. 6. Microhardness values of welds.

filler wire or base metal is strong. The oxygen potential is estimated by using Eq. (1) and the values are tabulated in Table 3.

$$O_p = O_2 + \mu CO_2 \quad (1)$$

where μ is the oxidizing factor, μ is taken as 0.7 as per the existing literatures [20,21].

3.2. Ferrite percentage

The ferrite percentages obtained using Fischer-feritscope MP30 are tabulated in Table 4 and plotted in Figs. 4a and 4b. From Fig. 4a as the percentage of CO₂ increases the ferrite percentage is found to be decreasing. This can be attributed to the presence of carbon which is an austenitic stabilizer. Austenitic area widens and ferrite percentage reduces as a result of increase in CO₂ percentage in the shielding gas. The increase of CO₂ in the shielding gas slows down the solidification rate and it can also reduce the ferrite percentage. This result is in line with Liao and Chen [1]. But the ferrite percentage of welds using 75% Ar + 23% CO₂ + 2% O₂ and 70% Ar + 25% CO₂ + 5% O₂ are not following the trend. This may be because the decomposition of CO₂ is retarded by oxygen in the mixtures [4].

Chemical compositions of the weld metals are found from spectro chemical analysis and they are tabulated in Table 5. The EDAX spectra of the welds were shown in Fig. 5. The Cr_{req} and Ni_{req} are found for base metal, filler wire and welds by using Eqs. (2) and (3) and the values are tabulated in Table 5.

$$Cr_{req} = Cr + 2(Si) + 1.5(Mo) + 5(V) + 5.5(Al) + 1.75(Nb) + 1.5(Ti) + 0.75(W) \quad (2)$$

$$Ni_{req} = Ni + Co + 0.5(Mn) + 0.3(Cu) + 25(N) + 30(C) \quad (3)$$

From Table 5 it is found that the carbon and nickel content in the weld metal increases with increasing of the CO₂ content in the

shielding gas. It is well known that nickel and carbon are strong austenite stabilizing elements. Therefore, the effect of CO₂ increase resulted in decreasing Cr_{req} and on the other hand, increasing of Ni_{req}. In addition to that, an increase of CO₂ percentage in the gas increases consumption of Cr, Si and Mn [22]. The amount of ferrite percentage in the weld metal is calculated using the Cr_{req} and Ni_{req} using WRC-92 diagram and tabulated in Table 6. From Table 6 it is clear that the measured ferrite percentage values are closer to predicted ferrite percentage values.

3.3. Microhardness

Microhardness test was conducted using Vickers micro hardness machine and hardness values were taken at weld zone, HAZ and base metal on both sides of the weld. Three readings were taken for each of them and the microhardness values are plotted in Fig. 6. From Fig. 6 it is observed that the base metal is having less hardness than the weld metal and the HAZ. This can be attributed to the fine grains found in weld metal and HAZ due to high temperature in those regions. Coarse grains are found in base metal. Microhardness values increase with increasing of ferrite percentage in the weld metal. Consequently, increase in CO₂ content in gases resulted in lowering hardness values of the weld metals [11]. But the hardness values of welds using 75% Ar + 23% CO₂ + 2% O₂ and 70% Ar + 25% CO₂ + 5% O₂ are not following the trend. This may be because the decomposition of CO₂ is retarded by oxygen in the mixtures [4].

3.4. Microstructures of the joints

The un-etched welds microstructure are shown in Fig. 7a–g. It is observed that the inclusion size and volume of inclusions are increased with increasing of CO₂ in the shielding gas. The major inclusions are oxides such as silicon oxides, and manganese oxides.

Typical microstructures of welds prepared under different shielding gases are shown in Figs. 8–14. Both dentritic and lathy ferrite morphologies were seen in the microstructures. It is clear that dentritic morphology is obtained by peritectic solidification while lathy ferrite is obtained by dissolution of ferrite during cooling [23]. Ferrite volume fraction decreases by increasing the amount of CO₂ in the shielding gas [4]. It is observed that the microstructures exhibit dendrite nature and dendrite becomes coarser when CO₂ increases in the shielding gas.

3.5. Impact properties of welds

The Charpy V notch impact test was conducted at 25 °C (room temperature), –100 °C and –196 °C temperatures. The average values obtained are presented in Table 7 and plotted in Fig. 15a. From Table 7 it can be observed that with decrease in temperature and increase in CO₂ percentage toughness values are decreasing [4]. Figs. 8–14 show that all the weld metals contain delta ferrite and austenitic phases. It is known that austenite has an fcc structure and delta ferrite a bcc structure. Fcc metal has high notch toughness is almost independent of temperature. On the other hand, the notch toughness of bcc metal is strongly dependent on temperature [3]. The fracture morphology of impact tested specimens is shown in Figs. 16–18. From Figs. 16–18 it is observed that the fracture morphology is ductile rupture at room temperature and ductile rupture with a few cleavages at low temperatures. From Fig. 7a–g the inclusions were found in welds. Inclusions, which act as crack initiator sites, will degrade the notch toughness property [5]. The more oxide inclusions formed when the percentage of CO₂ increases causes the toughness values to decrease. The influence of oxygen potential on notch toughness at various temperatures is shown in Fig. 15b. It is obvious that notch toughness

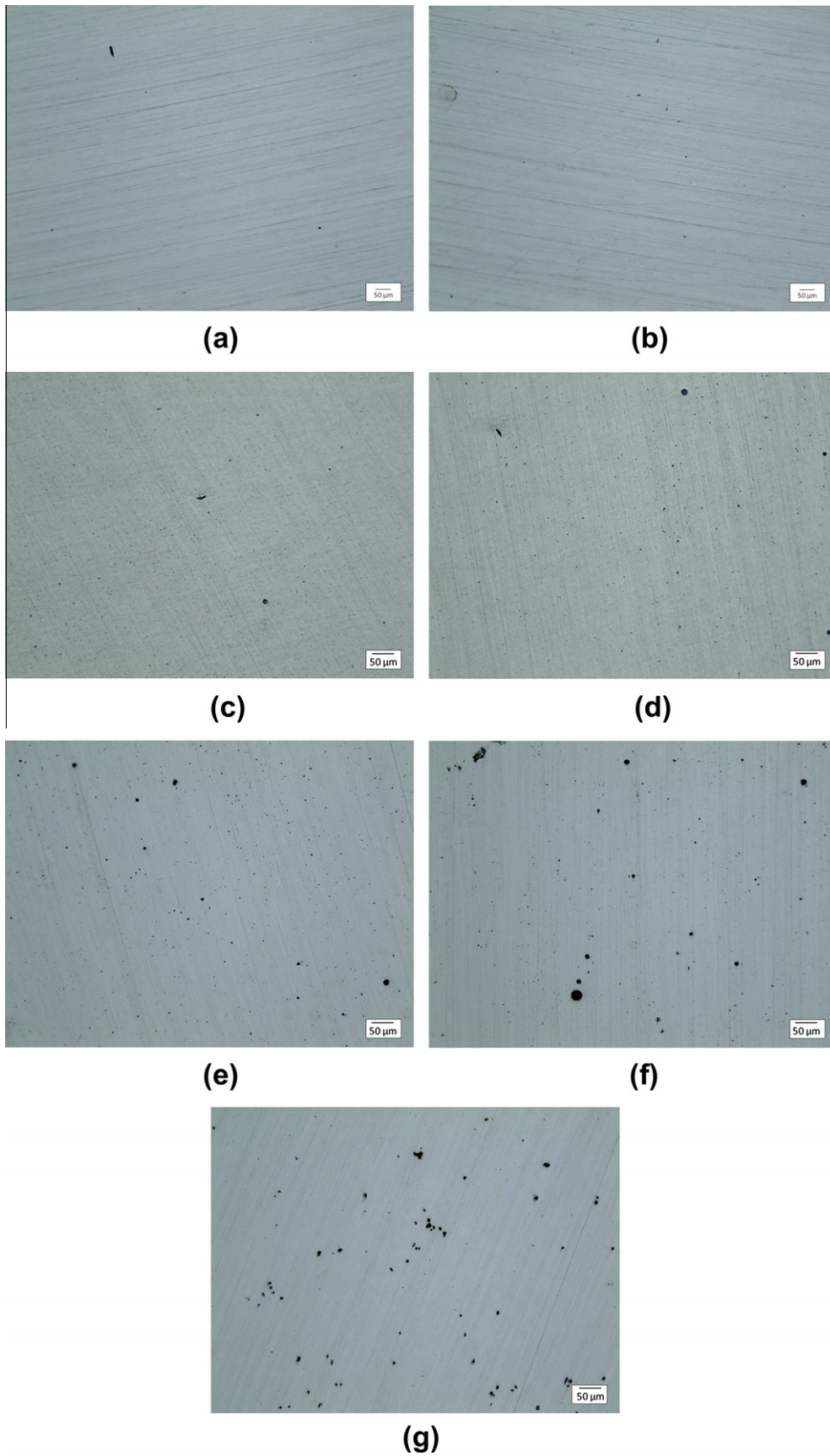


Fig. 7. (a–g) Un-etched microstructures of welds (a – 100% Ar, b – 95% Ar + 05% CO₂, c – 90% Ar + 10% CO₂, d – 80% Ar + 20% CO₂, e – 75% Ar + 23% CO₂ + 2% O₂, f – 70% Ar + 25% CO₂ + 5% O₂ and g – 100% CO₂).

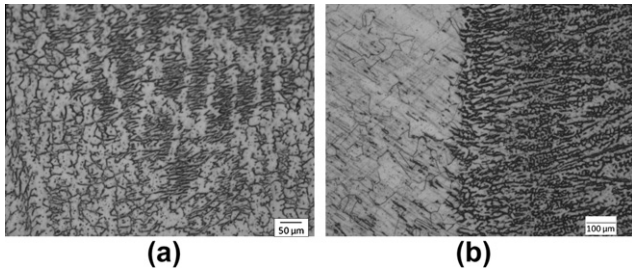


Fig. 8. Microstructure of welded specimen with 100% Ar (a – weld, and b – fusion zone).

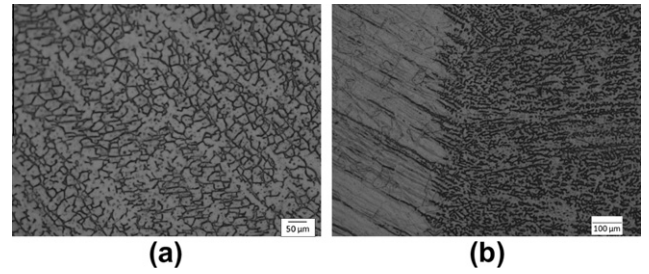


Fig. 12. Microstructure of welded specimen with 75% Ar + 23% CO₂ + 2% O₂ (a – weld, and b – fusion zone).

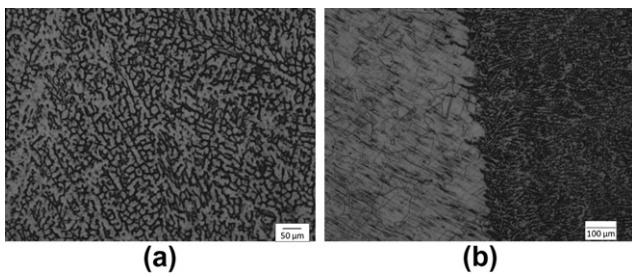


Fig. 9. Microstructure of welded specimen with 95% Ar + 05% CO₂ (a – weld, and b – fusion zone).

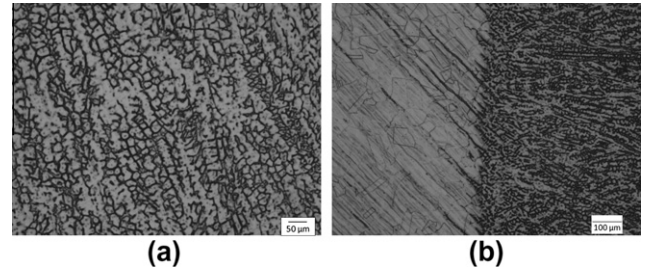


Fig. 13. Microstructure of welded specimen with 70% Ar + 25% CO₂ + 5% O₂ (a – weld, and b – fusion zone).

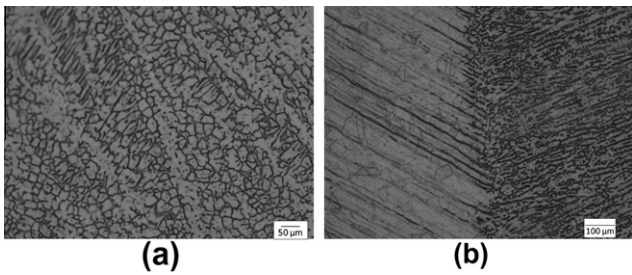


Fig. 10. Microstructure of welded specimen with 90% Ar + 10% CO₂ (a – weld, and b – fusion zone).

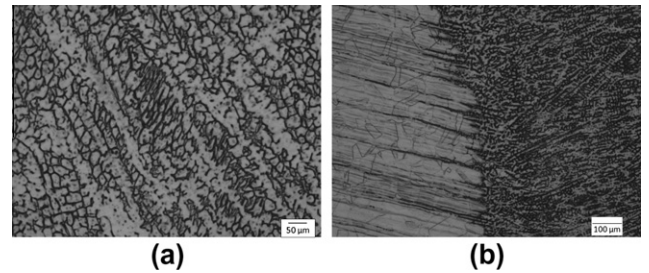


Fig. 14. Microstructure of welded specimen with 100% CO₂ (a – weld, and b – fusion zone).

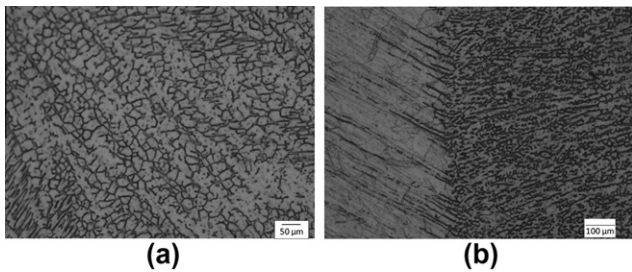


Fig. 11. Microstructure of welded specimen with 80% Ar + 20% CO₂ (a – weld, and b – fusion zone).

Table 7
Impact energy values of welds.

Shielding gas	Impact energy values (J) at different test temperatures		
	–196 °C	–100 °C	25 °C
100% Ar	40	54	80
95% Ar + 05% CO ₂	39	52	76
90% Ar + 10% CO ₂	38	50	72
80% Ar + 20% CO ₂	36	48	70
75% Ar + 23% CO ₂ + 2% O ₂	37	49	71
70% Ar + 25% CO ₂ + 5% O ₂	36	48	72
100% CO ₂	35	46	60

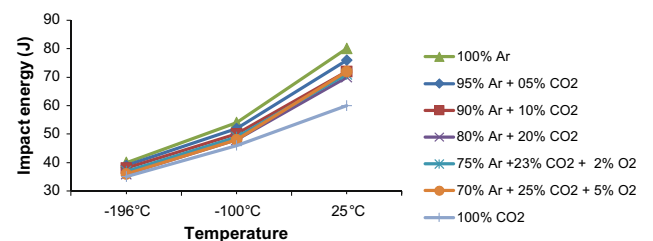


Fig. 15a. Effect of temperature on impact energy of welds.

drops as the oxygen potential increases at high testing temperatures while it is insensitive to oxygen potential at low testing temperatures [4].

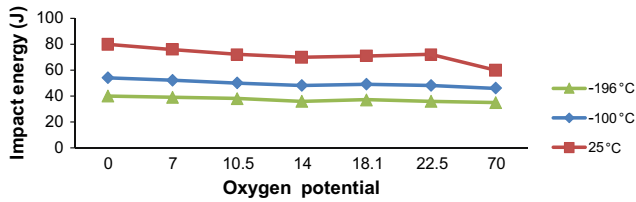


Fig. 15b. Effect of oxygen potential on impact energy of welds.

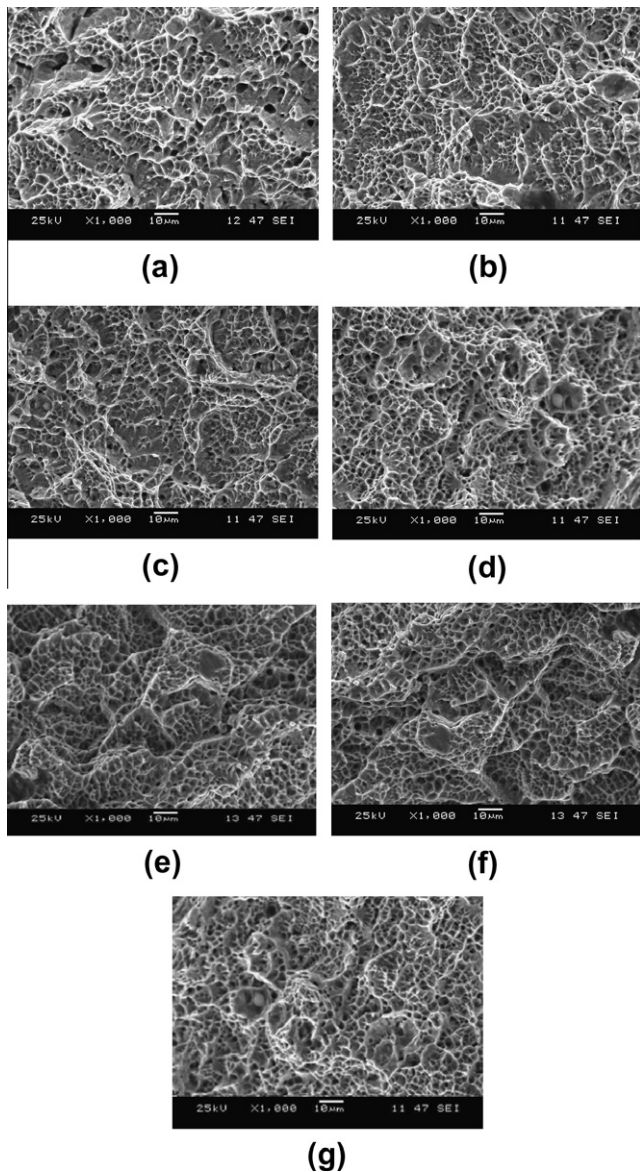


Fig. 16. (a–g) Fracture morphology (SEM image) of impact specimens –196 °C (a – 100% Ar, b – 95% Ar + 05% CO₂, c – 90% Ar + 10% CO₂, d – 80% Ar + 20% CO₂, e – 75% Ar + 23% CO₂ + 2% O₂, f – 70% Ar + 25% CO₂ + 5% O₂ and g – 100% CO₂).

3.6. Bend test

Face bend tests were performed to check the ductility of weld. The specimens after face bend tests are shown in Fig. 19 and no cracks or fissures were seen after bend test and ductility was retained as it is evident that the ductility of the material was found to be retained.

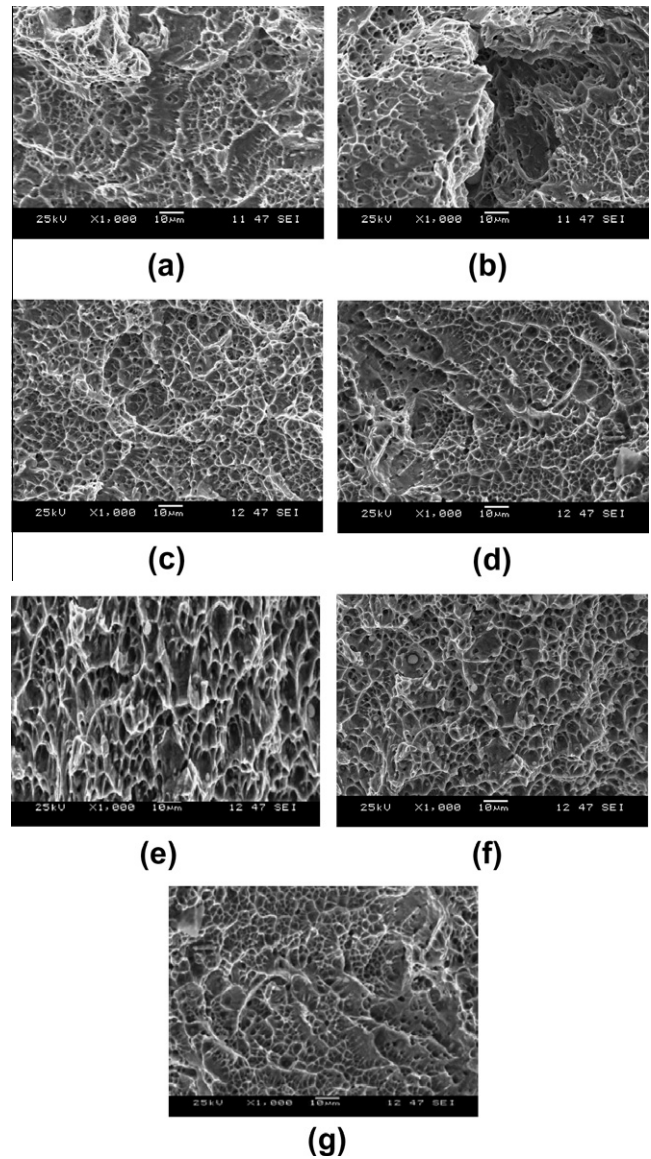


Fig. 17. (a–g) Fracture morphology (SEM image) of impact specimens at –100 °C (a – 100% Ar, b – 95% Ar + 05% CO₂, c – 90% Ar + 10% CO₂, d – 80% Ar + 20% CO₂, e – 75% Ar + 23% CO₂ + 2% O₂, f – 70% Ar + 25% CO₂ + 5% O₂ and g – 100% CO₂).

4. Conclusions

In this study, 316L (N) austenitic stainless steel was welded by flux cored arc welding with various shielding gases. The following conclusions are drawn:

1. Usage of various shielding gas mixtures found to affect the mechanical and metallurgical properties.
2. As the carbon dioxide percentage increases in the shielding gas mixture the austenitic area in the weld metal is widened and caused decrease in ferrite percentage. But when oxygen is added, the same trend is not followed because the decomposition of CO₂ is retarded by oxygen in the shielding gas mixtures.
3. Micro hardness values are higher in weld zone than in HAZ and base metal. The hardness values decreased with an increase of carbon dioxide in the shielding gas mixtures.

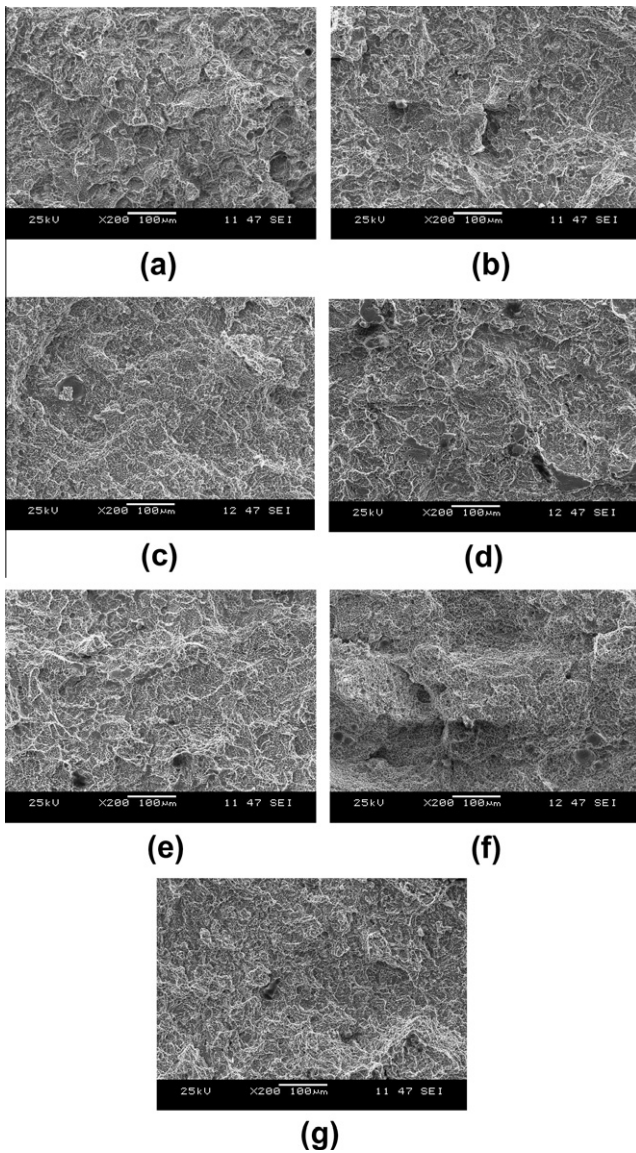


Fig. 18. (a–g) Fracture morphology (SEM image) of impact specimens at 25 °C (a – 100% Ar, b – 95% Ar + 05% CO₂, c – 90% Ar + 10% CO₂, d – 80% Ar + 20% CO₂, e – 75% Ar + 23% CO₂ + 2% O₂, f – 70% Ar + 25% CO₂ + 5% O₂ and g – 100% CO₂).

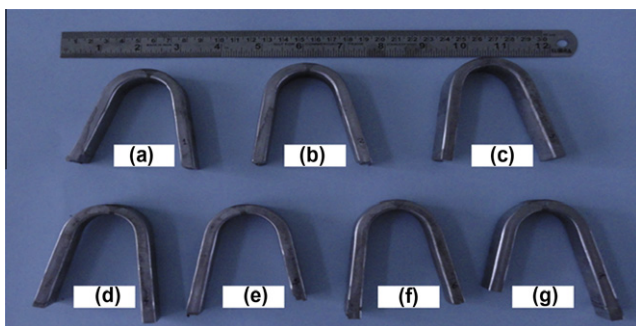


Fig. 19. (a–g) Specimens after bend test (a – 100% Ar, b – 95% Ar + 05% CO₂, c – 90% Ar + 10% CO₂, d – 80% Ar + 20% CO₂, e – 75% Ar + 23% CO₂ + 2% O₂, f – 70% Ar + 25% CO₂ + 5% O₂ and g – 100% CO₂).

4. The oxide inclusions formed with the increase in percentage of carbon dioxide in the shielding gas mixtures caused the toughness values to decrease.
5. No cracks or fissures are seen after bend test and ductility is retained.

References

- [1] Liao MT, Chen WJ. A comparison of gas metal arc welding with flux-cored wires and solid wires using shielding gas. *Int J Adv Manuf Technol* 1999;15(1):49–53.
- [2] Fischer GJ, Maciag RJ, The wrought stainless steels. In: Peckner D, Bernstein IM, editors. *Handbook of stainless steels*, McGraw-Hill, New York, NY, USA, vol. 1; 1977, pp. 1.1–1.9.
- [3] Dieter GE. *Mechanical metallurgy*. London: McGraw-Hill; 1988.
- [4] Liao MT, Chen WJ. The effect of shielding-gas compositions on the microstructure and mechanical properties of stainless steel weldments. *Mater Chem Phys* 1998;55:145–51.
- [5] Yılmaz R, Tümer M. the effect of shielding gases on the microstructure and toughness of stainless steels weldments by FCAW. In: *Annual assembly and international conference of the international institute of welding*, 11–17 July, AWST 10/85; 2010.
- [6] Mukhopadhyay S, Pal TK. Effect of shielding gas mixture on gas metal Arc Welding of HSLA steel using solid and flux-cored wires. *Int J Adv Manuf Technol* 2006;29:262–8.
- [7] Aloraier A, Ibrahim R, Thomson P. FCAW process to avoid the use of post weld heat treatment. *Int J Press Vessels Pip* 2006;83:394–8.
- [8] Mostafa NB, Khajavi MN. Optimisation of welding parameters for weld penetration in FCAW. *J Achievement Mater Manuf Technol* 2006;16(1–2):132–8.
- [9] Karadeniz Erdal, Ozsarac Ugur, Yildiz Ceyhan. The effect of process parameters on penetration in gas metal arc welding processes. *Mater Des* 2007;28:649–56.
- [10] Arivazhagan B, Sundaresan S, Kamaraj M. A study on influence of shielding gas composition on toughness of flux-cored arc weld of modified 9Cr 1Mo (P91) steel. *J Mater Process Technol* 2009;209:5245–53.
- [11] Ebrahimnia Mohamad, Goodarzi Massoud, Nouri Meisam, Sheikhi Mohsen. Study of the effect of shielding gas composition on the mechanical weld properties of steel ST 37–2 in gas metal arc welding. *Mater Des* 2009;30:3891–5.
- [12] Kang BY, Yarlagadda Prasad KDV, Kanga MJ, Kim HJ, Kim IS. The effect of alternate supply of shielding gasses in austenite stainless steel GTA welding. *J Mater Process Technol* 2009;209:4722–7.
- [13] Durgutlu Ahmet. Experimental investigation of the effect of hydrogen in argon as a shielding gas on TIG welding of austenitic stainless steel. *Mater Des* 2004;25:19–23.
- [14] Galloway Alexander, McPherson Norman. The effect of shielding gas composition on weld metal nitrogen retention in 316LN austenitic stainless steel. *Weld Cutting* 2006;5(4):225–30.
- [15] Jonsson J, Murphy PG, Zeckely AB. Influence of oxygen additions on argon shielded gas metal arc welding processes. *Weld J* 1995;74(2):48s–58s.
- [16] Subramaniam DR, White S. Effect of shield gas composition on surface tension of steel droplets in a gas-metal-arc welding arc. *Metall Mater Trans B* 2001;32B(2):313–8.
- [17] Pires RM, Quintino I, Miranda L. Analysis of the influence of shielding gas mixtures on the gas metal arc welding metal transfer modes and fume formation rate. *Mater Des J* 2006;28(5):1623–31.
- [18] Guile AE. The electric arc. In: Lancaster JF, editor. *The physics of welding*. Pergamon Press; 2001. p. 120–45.
- [19] ASM Handbook. *Metallography and microstructures*. 9th ed. Metals Park Ohio: ASM International; 1992. p. 282–90.
- [20] Stenbacka N, Persson KA. Shielding gases for gas metal arc welding. *Weld J* 1989;68(11):41–7.
- [21] Kobayashi T, Sugiyama T. The effect of shielding gas composition on the characteristics of stainless steel weld metal. *IIW Doc.XIZ-E-33-82.XII-B-25-82*; 1982.
- [22] Bundinski KG, Bundinski MK. *Stainless steels*. Eng Mater. 1999:455–61[6th ed].
- [23] Brooks JA, Thompson AW. Microstructural development and solidification cracking susceptibility of austenitic stainless steel welds. *Int Metall Rev* 1991;36:16.